G Model
CIRP-1535; No. of Pages 4

ARTICLE IN PRESS

CIRP Annals - Manufacturing Technology xxx (2016) xxx–xxx

Contents lists available at ScienceDirect

CIRP Annals - Manufacturing Technology

journal homepage: http://ees.elsevier.com/cirp/default.asp

Modelling of real area of contact between tool and workpiece in metal forming processes including the influence of subsurface deformation

Chris V. Nielsen [a,*], Paulo A.F. Martins (2)[b], Niels Bay (1)[a]

[a] *Department of Mechanical Engineering, Technical University of Denmark, 2800 Kgs. Lyngby, Denmark*
[b] *IDMEC, Instituto Superior Tecnico, Universidade de Lisboa, 1049-001 Lisbon, Portugal*

ARTICLE INFO

Keywords:
Metal forming
Friction
Real contact area

ABSTRACT

New equipment for testing asperity deformation at various normal loads and subsurface elongations is presented. Resulting real contact area ratios increase heavily with increasing subsurface expansion due to lowered yield pressure on the asperities when imposing subsurface normal stress parallel to the surface. Finite element modelling supports the presentation and contributes by extrapolation of results to complete the mapping of contact area as function of normal pressure and one-directional subsurface strain parallel to the surface. Improved modelling of the real contact area is the basis for estimating friction in the numerical modelling of metal forming processes.

1. Introduction

Among mechanisms in frictional sliding in metal forming, Bowden and Tabor [1] identified shearing of layers due to adhesion and cold welding between two surfaces and dragging or ploughing of a harder material through a softer material. Wanheim and Abildgaard [2] later added plastic waves in the softer material as an additional mechanism.

Bowden and Tabor [1] described the influence of asperity contact on friction, and observed that the linearity between normal pressure and friction in Amontons–Coulomb's model disappears when the real contact area becomes large. This was solved by Orowan [3] in modelling of rolling by applying the shear flow stress as an upper limit, and refined by the suggestion of a smooth transition by Shaw et al. [4].

Another important remark by Bowden and Tabor [1] is that friction cannot be regarded as a pure surface effect. Plastic bulk deformation influences the formation of contact area and hence friction. Fogg [5] observed during stretch forming, where subsurface deformation is present, that the real area of contact increases with bulk deformation due to the reduction of yield pressure when overlaid by tensile stresses.

The real area of contact, which explains the smooth transition suggested by Shaw et al. [4], has been investigated by slip-line analysis by Wanheim and Bay [6], who determined real area of contact as function of normal pressure by assuming regular asperities in contact with a smooth rigid tool under plane strain deformation. Wilson and Sheu [7] used upper bound analysis to set up a model for longitudinal asperities in rolling.

The mentioned theoretical models assume no subsurface deformation, and miss therefore one of the mechanisms influencing the formation of real contact area. Sutcliffe [8] developed a slip-line field, by combination of the field for equidistant indenters and the field for uniform deformation, for the analysis of real contact area as function of both normal pressure and subsurface deformation.

While Sutcliffe [8] was able to include subsurface deformation in his slip-line analysis, he was not able to include asperity interaction upon deformation as Wanheim and Bay [6] did, and on the contrary, they were not able to handle subsurface deformation. As far as the authors are aware, there is still no existence of a slip-line field that can handle both. Another limitation of slip-line analysis is the absence of strain hardening, although Bay [9] extended the analysis by including strain hardening in an average sense, and Sutcliffe [8] also gave an estimate of the effect of strain hardening.

These limitations call for the advantages of numerical analysis, although they cannot give direct analytical expressions. Makinouchi et al. [10] analyzed three asperities with free sides by elasto-plastic finite element analysis, where it was possible to include strain hardening. Later, the model was extended by Ike and Makinouchi [11] to five asperities and also single asperities with periodic boundary conditions. They were able to analyze different levels of subsurface deformation with their models. Another study was made by Korzekwa et al. [12], who simulated asperity deformation under different straining directions. They included strain hardening in an average sense. Lately, Wang et al. [13] derived a friction model based on a five-asperity model, where bulk deformation was also included.

Nielsen et al. [14] focused on the influence of strain hardening of the workpiece material for various normal pressures and presented an analytical expression for the real contact area as function of normal pressure and the strain hardening exponent.

* Corresponding author.
E-mail address: cvni@mek.dtu.dk (C.V. Nielsen).

http://dx.doi.org/10.1016/j.cirp.2016.04.126
0007-8506/© 2016 CIRP.

This study was performed without subsurface deformation, and this is what the present paper adds to these previous simulations.

The aim of the present paper is to show the real contact area ratio as function of subsurface deformation and normal pressure for a strain hardening material in terms of experiments and numerical simulations. The analysis covers compressive as well as tensile subsurface deformation, thereby covering the complete range of predominant stress distributions in metal forming processes, where friction modelling is required.

2. Experimental setup

Flattening of model asperities is conducted under different levels of normal pressure q and subsurface longitudinal strain ε_l. Fig. 1 shows two types of test specimens that are used. The bone shaped specimen in Fig. 1a is designed for longitudinal tension, while the specimen in Fig. 1b is designed for longitudinal compression. Both specimens have regular, two-dimensional model asperities perpendicular to the direction of subsurface deformation made by wire-cut EDM. They have triangular cross-section and are scaled up in size to allow clear detection of the real contact area ratio, and they are modelled by a flank angle $\gamma = 10^\circ$ and a wavelength $t = 1.5$ mm.

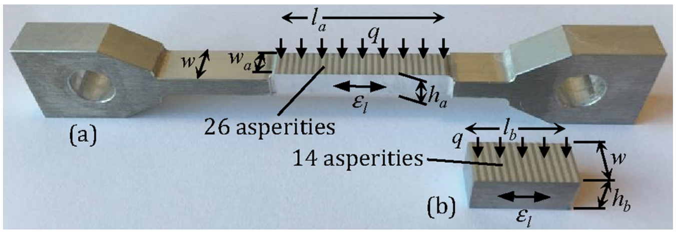

Fig. 1. Test specimens with model asperities to be flattened under normal pressure q while experiencing subsurface longitudinal strain ε_l due to (a) longitudinal tension or (b) longitudinal compression. Dimensions are $w = 10$ mm, $w_a = 7$ mm, $l_a = 39$ mm, $l_b = 21$ mm, $h_a = 10$ mm and $h_b = 9.5$ mm.

The workpiece material is aluminium A1050 with a Hollomon flow stress curve:

$$\sigma = C\epsilon^n = 140\epsilon^{0.21}\ [\text{MPa}] \quad (1)$$

obtained by simple upsetting tests. In Eq. (1), C is the strength coefficient and n is the strain hardening exponent. In the asperity flattening experiments, fine zinc stearate powder was used for lubrication. It was rubbed to the workpiece surface after pickling in a NaOH bath. The zinc stearate was applied in a thin layer to minimize the possibility of entrapment in the valleys during asperity flattening, which would diminish the formation of real contact between workpiece and tool.

The experiments were conducted in a channel tool installed for asperity flattening under tensile subsurface deformation as shown in Fig. 2 or compressive subsurface deformation as shown in Fig. 3.

The testing procedure in the experiments shown in Fig. 2 is:

- The test specimen (1) is placed in the channel tool (2) for aligning purposes and for support on the bottom.
- The punch (3) moves down to apply a normal force on the asperities. The force is kept constant throughout the test and the final normal pressure q is calculated based on the final dimensions of the test specimen.
- Longitudinal subsurface strain is induced by tension through the position controlled axis (4), while the other end of the specimen is clamped by the shoe (5) and the chock preventing movement of this end (6).
- Steady state sliding is obtained by removing the chock (6), which allows free movement of the specimen including the clamping shoe (5) to the left by the position controlled axis (4).

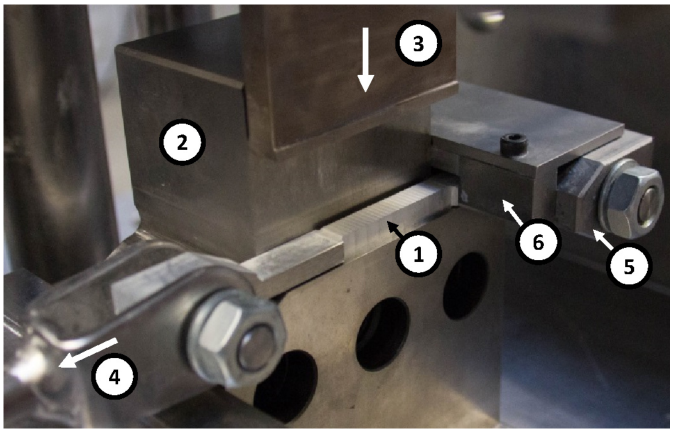

Fig. 2. Experimental setup for asperity flattening under tensile subsurface deformation showing (1) test specimen, (2) channel tool consisting of a bottom and two sides (of which one was removed for taking the photograph), (3) punch, (4) position controlled axis, (5) clamping shoe, and (6) removable chock.

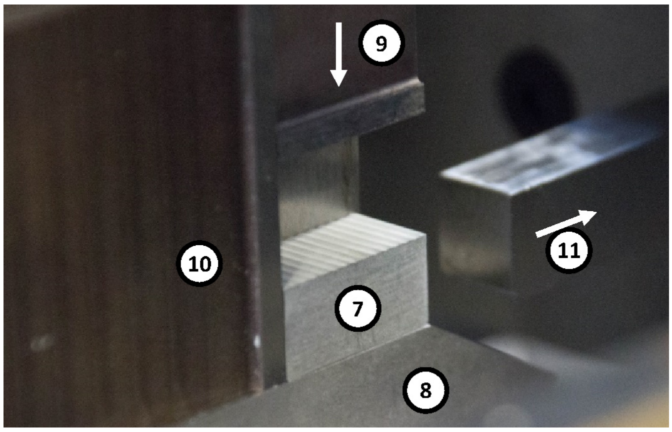

Fig. 3. Experimental setup for asperity flattening under compressive subsurface deformation showing (7) test specimen, (8) channel tool consisting of a bottom and two sides (of which one was removed for taking the photograph), (9) punch, (10) stationary tool, and (11) position controlled counter pressure tool.

The testing procedure in the experiments with compressive subsurface deformation as in Fig. 3 is:

- The test specimen (7) is placed in the channel tool (8) to ensure plane strain deformation.
- The stationary tool (10) impedes movement in one direction while movement to the opposite end is initially hindered by having the position controlled counter pressure tool (11) in contact with the specimen.
- The punch (9) moves down to apply a normal pressure q on the workpiece asperities.
- The position controlled tool (11) is moved a certain distance to allow subsurface deformation of the specimen. This deformation happens under longitudinal compression as the workpiece is deformed against tool (11).

Plane strain deformation is ensured by the channel tool in Fig. 3. This is not the case in the experiments shown in Fig. 2, since, if the specimen has the width of the channel tool and is expanded towards the sides, friction will hinder the elongation of the asperity region, and the result will instead be necking in front of the test zone. To avoid necking, the asperity region is made narrower than the channel tool as it can be seen in Fig. 1a ($w_a < w$). In absence of friction between the specimen and the bottom tool (part of the channel tool (2)) and the punch (3), this would result in a plane stress state. Presence of friction does however alter the stress state from pure plane stress. In some cases, as it will be discussed in